Baltic Astronomy, vol. 15, 461–469, 2006.

A SURVEY OF COMPACT STAR CLUSTERS IN THE SOUTH-WEST FIELD OF THE M 31 DISK. UBVRI PHOTOMETRY

D. Narbutis[1], V. Vansevičius[1], K. Kodaira[2], I. Šablevičiūtė[1], R. Stonkutė[1,3] and A. Bridžius[1]

[1] *Institute of Physics, Savanorių 231, Vilnius LT-02300, Lithuania*
wladas@astro.lt
[2] *The Graduate University for Advanced Studies (SOKENDAI), Shonan Village, Hayama, Kanagawa 240-0193, Japan*
[3] *Vilnius University Observatory, Čiurlionio 29, Vilnius LT-03100, Lithuania*

Received 2006 September 15; accepted 2006 September 30

Abstract. We present the results of *UBVRI* broad-band aperture CCD photometry of 51 compact star clusters located in the South-West part of the M 31 disk. The mean rms errors of all measured star cluster colors are less than 0.02 mag. In color vs. color diagrams the star clusters show significantly tighter sequences when compared with the photometric data from the compiled catalog of the M 31 star clusters published by Galleti et al. (2004).

Key words: galaxies: individual (M 31) – galaxies: star clusters

1. INTRODUCTION

Recently Kodaira et al. (2004, hereafter Paper I) conducted a survey of compact star clusters in the South-West part of the M 31 disk finding 101 prominent compact objects. In the present paper we investigate part of these clusters using the Local Group Galaxy Survey mosaic images of M 31, produced by Massey et al. (2006). These images were used to perform *UBVRI* broad-band (R and I bands in the Cousins system) aperture photometry of 49 compact (KWC) and 2 compact emission (KWE) objects from Paper I. The KWC list was supplemented by two KWE objects satisfying the magnitude limit, $V < 19$, which was generally applied for the selection of the KWC objects. The structural parameters of these star clusters will be presented by Šablevičiūtė et al. (2007, in preparation)

2. DATA

We used publicly available[1] stacked U, B, V, R and I band mosaic images of M 31 (fields F6, F7, F8, F9), calibrated by Massey et al. (2006), which overlap with the field studied in Paper I. The mosaic camera used by Massey et al. (2006) consists of eight CCDs. Each CCD chip covers $9' \times 18'$ field and has an individual set of color equations. The observations and data reductions are described in detail by Massey et al. (2006).

We considered mosaic images, clean from cosmic rays and cosmetically, to be

[1] See http://www.lowell.edu/users/massey/lgsurvey.html

more preferable for aperture star cluster photometry than individual exposures. The dithering pattern of five individual exposures for each field is the same with maximum shifts up to $1'$ in respect to the first exposure. Exceptions are U-band observations in the F9 field, which has 6 individual exposures. Massey et al. (2006) do not recommend straightforward use of their mosaic images for precise photometry, therefore, we treat each CCD chip area on the stacked mosaic image separately, with special care for objects residing on different CCDs in individual exposures.

2.1. Point-spread function unification

Mosaic images employed for aperture photometry have different widths of stellar point-spread functions (PSF). Full width at half maximum (FWHM) ranges from $0.7''$ to $1.3''$ (pixel size is $0.27''$). Four mosaic images have coordinate dependent PSFs with FWHM varying more than $0.2''$ and reaching maximum of $0.3''$ for the field's F7 I-band mosaic image. Consequently, this could lead to variable aperture corrections and star cluster color bias when measured with aperture sizes as small as $\sim 3''$ used in this study. Therefore, we applied the DAOPHOT package of IRAF program system (Tody 1993) to compute PSF for every mosaic image. The widest PSF (FWHM $= 1.3''$) was convolved with the Gaussian kernel producing the reference PSF of FWHM $= 1.5''$. IRAF's $psfmatch$ procedure was employed to compute required convolution kernels for individual mosaic images in respect to the reference PSF. The kernels were symmetrized by replacing cores with the best fitting Gaussian profiles, and the kernel wings with the best fitting exponential profiles truncated at $3.5''$.

IRAF's *convolve* procedure was employed to produce mosaic images possessing the unified PSF (FWHM $= 1.5''$). Finally, we achieved uniform and coordinate-independent PSF across all convolved images. The maximum difference of the aperture corrections among different photometric passband and observed field mosaic images is less than 0.02 mag. The convolved images were photometrically calibrated and used for star cluster photometry.

2.2. Photometric calibration

We carefully selected well-isolated stars from Massey et al. (2006) Table 4 for calibration of the $UBVRI$ magnitudes. The selection criteria were as follows: the photometric error $\sigma < 0.03$ mag and the number of observations >3 in each passband. The total fluxes of the calibration stars were measured by employing IRAF's *phot* procedure through a circular aperture of $3.0''$ in diameter and by applying the same aperture correction of 0.27 mag for all mosaic images.

Massey et al. (2006) in Table 2 provide color terms for individual CCD chips of their mosaic camera and color equations. We solved those equations by fitting photometric zero-points for every individual CCD chip of the mosaic images. Typically 80 (ranging from 20 to 140) calibration stars per chip were used. The final errors of the derived zero-points are less than 0.01 mag with typical fitting rms <0.03 mag for the I-band and <0.02 mag for other passbands.

Color equations given by Massey et al. (2006) supplemented with derived zero-points were used to transform instrumental magnitudes to the standard system. Reliability and accuracy of calibrations were discussed by Massey et al. (2006) and Narbutis, Stonkutė & Vansevičius (2006).

3. RESULTS

Aperture photometry was carried out for 51 compact objects, selected from Paper I, by employing the XGPHOT package of IRAF. All objects are free of visible defects on mosaic images. Aperture centers were determined basing on the fit of star cluster luminosity distribution peaks on V-band mosaic images. In order to avoid star cluster photometry contamination by background objects in the crowded fields (see Paper I, Figures 5 and 6), we decided to use individual small size circular (for the objects KWC13, KWC20 and KWC31 – elliptical) apertures, indicated in Table 1. Sky backgrounds were measured in individual circular or elliptical annuli (typical width $4''$), centered on the objects. For some star clusters, residing on largely variable sky background, the annuli were not centered on the objects. These star clusters are noted by word "sky" in Table 1.

Our sample consists of 27 and 24 star clusters having two and three independent measurements on different mosaic images (consequently different CCDs), respectively. Measured star clusters are relatively bright objects, therefore, photon noise is virtually negligible and photometric accuracy of the catalog is limited by the photometric calibration procedure. For the star clusters located in the mosaic image areas, stacked from different CCDs, we additionally used color equations of corresponding CCDs and performed independent transformations to the standard system. V-band magnitudes and colors, determined in different fields (F6–F9), were averaged by assigning smaller weights to the measurements performed on the mosaic image areas, stacked from different CCDs. The final catalog is provided in Table 1, with corresponding rms errors indicated. We artificially set the lower accuracy limit to 0.01 mag, because of possible photometry zero-point errors of different mosaic images. The mean accuracy of all colors is better than 0.02 mag.

In order to check the aperture size and centering error effects on color accuracy we measured all objects, setting aperture sizes larger and smaller than the standard aperture size by 10 %, and shifting position of the standard aperture in both directions of the RA and Dec coordinates by $0.15''$, which corresponds to the average coordinate discrepancy among different passband mosaic images. Distributions of the measured star cluster color differences were found to be consistent with the Gaussian distribution (rms scatter <0.007 mag), and no systematic bias was noticed. Upper limit of possible color differences due to aperture size or center variation larger than 0.015 mag (all of them do not exceed 0.025 mag) is inherent to some colors of the clusters KWC09, KWC15, KWC16, KWC24, KWC44, KWC46, KWC47, KWE33 and KWE52. Their corresponding rms errors in Table 1 are marked by asterisks.

The catalog of 51 M 31 compact star clusters presented in Table 1 has the following columns:

1 – KWC or KWE number of a star cluster as defined in Paper I;

2–3 – RA and Dec (J2000.0) are coordinates in the V-band mosaic image coordinate system of field F7 (Massey et al. 2006) given in degrees;

4 – V aperture magnitude (note that it is not the total magnitude);

5–8 – $U-B$, $B-V$, $V-R$, $R-I$ colors with corresponding rms errors in the line below;

9 – the number of independent measurements (n) in different fields;

10 – diameter of circular aperture or major axis length of elliptic aperture (Ap) in arcseconds;

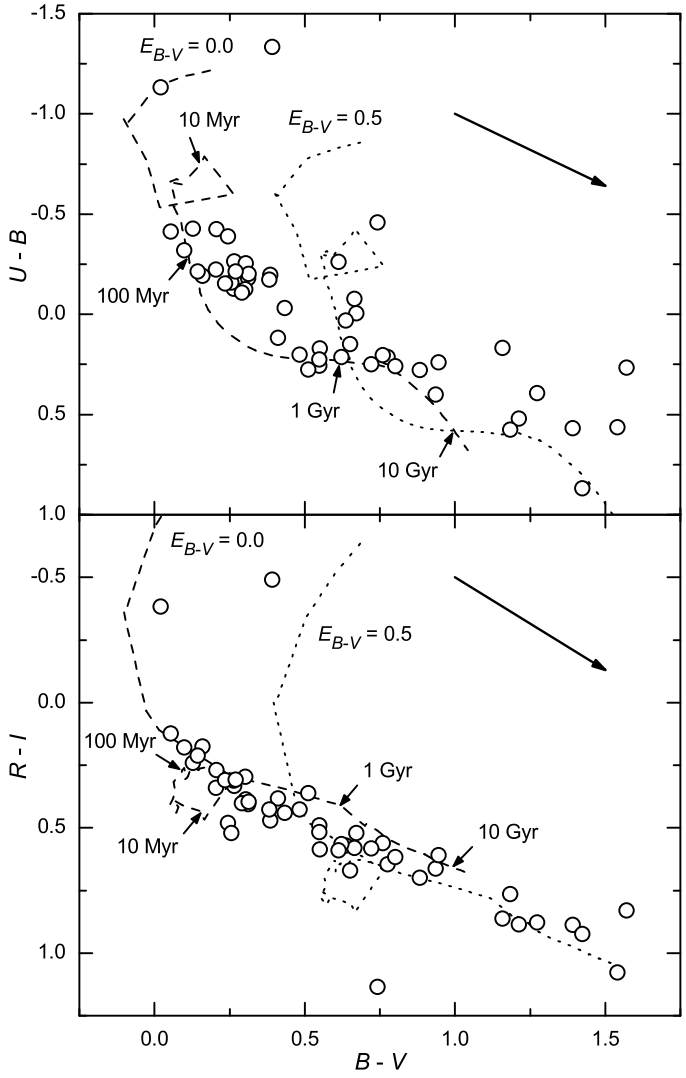

Fig. 1. Color-color diagrams of the 51 star clusters (open circles; Table 1). PÉGASE SSP models ($Z = 0.02$, age range from 1 Myr to 15 Gyr) with $E_{B-V} = 0$ (dashes) and $E_{B-V} = 0.5$ (dots) are over-plotted. The reddening vectors, corresponding to the standard Milky Way extinction law, are indicated. Small arrows indicate the SSP ages of 10 Myr, 100 Myr, 1 Gyr and 10 Gyr.

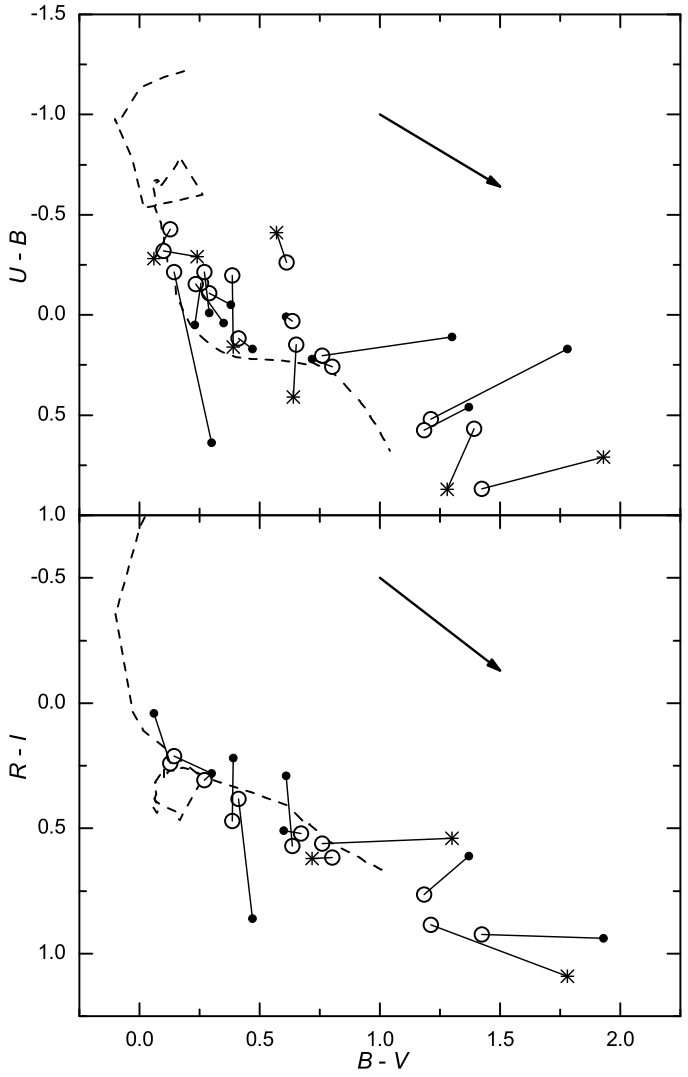

Fig. 2. Color-color diagrams of the corresponding star clusters taken from the catalog presented in Table 1 (open circles) and from Galleti et al. (2004) (dots – CCD photometry; asterisks – photographic photometry). Lines connect the same object in both catalogs. SSP models and reddening vectors are the same as in Fig. 1. In total 18 and 12 star clusters are shown in the top and bottom panels, respectively.

Table 1. *UVBRI* photometry catalog of the M 31 compact star clusters.

Cluster	RA(2000)	Dec(2000)	V	$U-B$	$B-V$	$V-R$	$R-I$	n	Ap	Note
KWC01	10.04577	40.60326	18.498	–0.426	0.206	0.223	0.269	3	3.0	...
			0.012	0.020	0.010	0.010	0.010			
KWC02	10.05932	40.65581	18.824	–0.265	0.265	0.227	0.332	3	3.6	...
			0.024	0.010	0.018	0.011	0.013			
KWC03	10.06074	40.62242	18.566	–0.413	0.054	0.096	0.124	3	3.0	...
			0.010	0.023	0.011	0.010	0.010			
KWC04	10.06408	40.61515	18.590	–0.180	0.312	0.262	0.406	3	3.2	...
			0.025	0.024	0.016	0.011	0.010			
KWC05	10.06460	40.66653	18.486	–0.254	0.303	0.284	0.387	3	3.4	...
			0.010	0.022	0.010	0.010	0.010			
KWC06	10.07201	40.65136	18.125	–0.428	0.127	0.155	0.241	3	3.6	...
			0.010	0.013	0.010	0.010	0.010			
KWC07	10.07320	40.65556	18.560	–0.320	0.099	0.112	0.179	3	3.0	...
			0.010	0.027	0.015	0.010	0.010			
KWC08	10.07620	40.54577	18.559	0.116	0.411	0.293	0.383	3	3.6	...
			0.014	0.010	0.010	0.010	0.018			
KWC09	10.07855	40.52101	19.329	0.266	1.570	0.770	0.830	2	3.0	...
			0.022	0.035*	0.014*	0.011	0.024			
KWC10	10.08099	40.62479	18.687	–0.197	0.385	0.332	0.470	3	3.0	...
			0.010	0.013	0.010	0.010	0.010			
KWC11	10.08302	40.51324	18.742	–0.193	0.159	0.142	0.175	2	3.4	...
			0.021	0.010	0.010	0.010	0.010			
KWC12	10.09631	40.51323	17.477	–0.005	0.671	0.465	0.521	2	6.8	...
			0.017	0.010	0.013	0.010	0.020			
KWC13	10.10304	40.63052	17.221	0.569	1.391	0.809	0.888	3	6.0	0.55, 50
			0.010	0.017	0.017	0.010	0.015			
KWC14	10.10351	40.81297	19.227	0.171	0.550	0.440	0.585	2	3.0	sky
			0.010	0.010	0.020	0.010	0.014			
KWC15	10.10370	40.81690	19.693	0.213	0.776	0.591	0.645	2	3.0	sky
			0.010	0.017*	0.024	0.011	0.012			
KWC16	10.10807	40.62813	19.326	0.168	1.158	0.778	0.862	3	3.0	...
			0.010	0.021*	0.023*	0.010	0.016			
KWC17	10.11374	40.75674	18.740	–0.224	0.205	0.238	0.341	2	3.0	...
			0.014	0.010	0.011	0.010	0.018			
KWC18	10.13581	40.83711	19.140	–0.127	0.264	0.230	0.311	2	3.0	...
			0.010	0.010	0.010	0.010	0.010			
KWC19	10.15227	40.67085	19.027	0.030	0.636	0.460	0.571	3	3.0	...
			0.016	0.010	0.010	0.010	0.010			
KWC20	10.15519	40.65408	19.144	–0.077	0.665	0.455	0.580	3	3.4	0.75, 120
			0.019	0.014	0.010	0.010	0.014			
KWC21	10.15569	40.81267	19.255	–0.126	0.302	0.223	0.297	2	3.0	...
			0.010	0.013	0.010	0.010	0.010			
KWC22	10.17370	40.64113	18.726	0.521	1.212	0.758	0.885	3	3.4	...
			0.011	0.013	0.010	0.015	0.014			

Table 1. Continued

Cluster	RA(2000)	Dec(2000)	V	$U-B$	$B-V$	$V-R$	$R-I$	n	Ap	Note
KWC23	10.17619	40.60127	19.226	0.203	0.759	0.469	0.560	3	3.0	...
			0.010	0.010	0.010	0.013	0.024			
KWC24	10.18421	40.74610	19.815	0.563	1.541	1.014	1.078	2	3.0	...
			0.010	0.017*	0.021*	0.010	0.010			
KWC25	10.19348	40.86130	19.182	–0.174	0.382	0.316	0.426	2	3.2	...
			0.010	0.010	0.010	0.011	0.015			
KWC26	10.20151	40.58503	18.406	–0.108	0.291	0.252	0.401	3	3.0	...
			0.010	0.010	0.010	0.012	0.011			
KWC27	10.20159	40.86619	18.620	–0.388	0.245	0.316	0.480	3	3.0	...
			0.012	0.025	0.010	0.010	0.010			
KWC28	10.20241	40.96009	19.280	0.257	0.548	0.396	0.490	2	3.0	sky
			0.010	0.020	0.010	0.010	0.014			
KWC29	10.20591	40.69223	18.283	0.258	0.801	0.501	0.617	2	3.4	...
			0.010	0.010	0.010	0.010	0.010			
KWC30	10.21459	40.55770	19.273	0.148	0.651	0.450	0.670	3	3.2	...
			0.010	0.022	0.010	0.013	0.021			
KWC31	10.21512	40.73504	17.982	–0.458	0.742	0.670	1.135	2	4.2	0.70, 30
			0.010	0.014	0.010	0.010	0.014			
KWC32	10.21786	40.89896	19.287	0.401	0.936	0.568	0.662	3	3.2	...
			0.010	0.022	0.011	0.010	0.012			
KWC33	10.21782	40.97817	19.450	0.213	0.622	0.447	0.565	2	3.0	sky
			0.010	0.020	0.010	0.010	0.011			
KWC34	10.22069	40.58883	18.878	0.277	0.882	0.576	0.699	3	4.4	...
			0.010	0.016	0.014	0.010	0.011			
KWC35	10.23960	40.74087	19.079	0.393	1.273	0.810	0.877	2	3.0	...
			0.010	0.010	0.010	0.010	0.018			
KWC36	10.27868	40.57474	19.146	–0.201	0.313	0.288	0.396	3	3.0	...
			0.011	0.021	0.020	0.010	0.022			
KWC37	10.28315	40.88356	18.700	0.239	0.945	0.584	0.608	3	3.0	...
			0.017	0.012	0.010	0.012	0.021			
KWC38	10.29172	40.96973	19.013	0.249	0.721	0.461	0.582	2	3.0	...
			0.010	0.017	0.010	0.010	0.017			
KWC39	10.30333	40.57155	18.104	–0.158	0.256	0.266	0.521	2	3.6	sky
			0.010	0.010	0.010	0.010	0.015			
KWC40	10.30768	40.56615	18.321	–0.155	0.234	0.216	0.310	2	3.6	...
			0.010	0.015	0.010	0.010	0.019			
KWC41	10.32568	40.73369	19.181	0.225	0.549	0.362	0.517	2	3.2	...
			0.010	0.010	0.010	0.010	0.010			
KWC42	10.32810	40.95436	17.666	0.869	1.423	0.830	0.923	2	4.0	...
			0.010	0.016	0.010	0.010	0.022			
KWC43	10.33723	40.98452	18.114	0.575	1.184	0.685	0.764	2	3.4	...
			0.010	0.023	0.010	0.010	0.010			
KWC44	10.35044	40.61307	18.687	–0.213	0.144	0.145	0.212	2	4.0	...
			0.010	0.010	0.010	0.010	0.027*			

Table 1. Continued

Cluster	RA(2000)	Dec(2000)	V	$U-B$	$B-V$	$V-R$	$R-I$	n	Ap	Note
KWC45	10.36251	40.69373	19.221	–0.032	0.433	0.341	0.440	2	3.0	...
			0.010	0.010	0.029	0.010	0.026			
KWC46	10.40363	40.79040	18.691	0.201	0.483	0.334	0.426	3	3.0	...
			0.014	0.018	0.017	0.010	0.014*			
KWC47	10.40855	40.56967	18.948	–0.263	0.612	0.393	0.590	2	3.0	...
			0.010	0.021*	0.010	0.017	0.010			
KWC48	10.41051	40.82676	19.293	0.276	0.512	0.327	0.362	3	3.0	...
			0.017	0.022	0.011	0.010	0.011			
KWC49	10.41184	40.68182	18.111	–0.214	0.270	0.238	0.308	2	3.0	...
			0.010	0.028	0.010	0.010	0.010			
KWE33	10.19922	40.98502	18.459	–1.335	0.392	0.294	–0.491	2	4.0	...
			0.010	0.031*	0.018	0.010	0.010*			
KWE52	10.41127	40.73314	18.793	–1.132	0.021	0.502	–0.384	2	3.6	...
			0.011	0.026*	0.010	0.010*	0.011*			

11 – notes (for elliptic apertures: ratio of minor to major axis and position angle of the major axis, calculated counterclockwise from the North direction; "sky" - sky background values measured in the annulus not centered on the objects).

Color-color diagrams of the compact star clusters from Table 1 are shown in Figure 1 with over-plotted simple stellar population (SSP) models of solar metallicity ($Z = 0.02$) computed with PÉGASE (Fioc & Rocca-Volmerange 1997). Default PÉGASE parameters and universal initial mass function (IMF) by Kroupa (2002) were applied. Reddening arrows are depicted by applying the color excess ratios of the standard extinction law (V-band extinction to color excess ratio, $A_V/E_{B-V} = 3.1$). Galactic interstellar extinction in the direction of the South-West part of the M 31 galaxy was estimated by employing NASA Extragalactic Database Galactic Reddening and Extinction Calculator, $E_{B-V} = 0.06$. However, star cluster photometry data, plotted in Figures 1 and 2, are not dereddened.

We compared our catalog data with the data from the compiled catalog published by Galleti et al. (2004; version V.2.0, May 2006)[2]. In total 27 star clusters were cross-identified (18 and 12 objects have $U-B$ and $R-I$ colors, respectively) and are shown in Figure 2. Our photometric data exhibit significantly smaller scatter in color-color diagrams, which is a result of homogeneous photometric survey of the M 31 galaxy performed by Massey et al. (2006) and individual apertures carefully chosen for each star cluster. Therefore, we conclude that accuracy of the measured aperture colors of the M 31 compact star clusters is satisfactory to be used for star cluster parameter (age, extinction, metallicity) determination basing on comparison with SSP models. Photometry data analysis of the measured compact clusters will be presented elsewhere (Vansevičius et al. 2007, in preparation).

ACKNOWLEDGMENTS. This work was financially supported in part by a Grant T-08/06 of the Lithuanian State Science and Studies Foundation. This

[2] See http://www.bo.astro.it/M31/

research has made use of the NASA/IPAC Extragalactic Database (NED) which is operated by the Jet Propulsion Laboratory, California Institute of Technology, under contract with the National Aeronautics and Space Administration, and of SAOImage DS9, developed by Smithsonian Astrophysical Observatory. We are thankful to Valdas Vansevičius for correcting the manuscript.

REFERENCES

Fioc M., Rocca-Volmerange B. 1997, A&A, 326, 950

Galleti S., Federici L., Bellazzini M., Fusi Pecci F., Macrina S. 2004, A&A, 416, 917

Kodaira K., Vansevičius V., Bridžius A., Komiyama Y., Miyazaki S., Stonkutė R., Šablevičiūtė I., Narbutis D. 2004, PASJ, 56, 1025

Kroupa P. 2002, Science, 295, 82

Massey P., Olsen K. A. G., Hodge P. W., Strong S. B., Jacoby G. H., Schlingman W., Smith R. C. 2006, AJ, 131, 2478

Narbutis D., Stonkutė R., Vansevičius V. 2006, Baltic Astronomy, 15, 471 (this issue)

Tody D. 1993, in *Astronomical Data Analysis Software and Systems II*, eds. R. J. Hanisch, R. J. V. Brissenden & J. Barnes, ASP Conf. Ser., 52, 173